

University of Illinois at Urbana-Champaign
Degree of Doctor of Physics



Drell-Yan at COMPASS rocks it!

Candidate: Robert Shannon Heitz

Supervisor: Prof. Matthias Grosse-Perdekamp

Supervisor: Prof. Caroline Riedl

To whom it may concern

Abstract

Dear Barbara Badelek, hereafter my abstract

Table of Contents

Chapter 1	Measurement of the Left Right Asymmetry in the Drell-Yan Process	1
1.1	Data Sample	1
1.1.1	Event Selection	1
1.1.2	Binning	4
1.2	Extraction of Asymmetries	4
1.2.1	Geometric Mean	4
1.2.2	Four Target Geometric Mean	6
1.3	Results	8
1.3.1	Comparison of results	9
1.4	Systematic Studies	9
1.4.1	Period Compatibility	9
1.4.2	False Asymmetries	12
1.4.3	Further False Asymmetry Effects	13
1.4.4	Left/Right Event Migration	14
Introduction	1
List of Figures	16
List of Tables	17
Chapter 2	References	18

Chapter 1

Measurement of the Left Right Asymmetry in the Drell-Yan Process

Introduction about L/R asym. In this Chapter.... Define AN

1.1 Data Sample

The data sample comes from the 2015 COMPASS Drell-Yan measurement where a 190 GeV/c π^- beam impinged on a transversely polarized NH_3 target. The stable data comes from July 8, through November 12 and is split into 9 periods lasting approximated 2 weeks each where each period consist of two sub-periods. To reduce systematics, the NH_3 was split into two oppositely polarized cells separated by 20 cm and the polarization of both cells was flipped between sub-periods. A summary of the data taking from each period is shown in table 1.1.

1.1.1 Event Selection

The cuts in the event selection were chosen to ensure the final state consisted of dimuons resulting from a pion collision in the transversely polarized target. The event selection was initial filtered from miniDSTs to μ DSTs using the criteria of at least two muons in the final state. The following event selection is performed on these μ DSTs where the events used come from the slot1 production. A summary of the number of events remaining after each cut is shown in table 1.2.

- Two oppositely charged particles from a common best primary vertex. The criteria for a primary vertex is any vertex with an associated beam particle. In case of multiple common vertices the best primary vertex was determined by CORAL tagging the vertex

Period	Sub-period	Polarization	First-Last run	Begin date	End date
W07	one	$\downarrow\uparrow$	259363 - 259677	July 9	July 15
	two	$\uparrow\downarrow$	259744 - 260016	July 16	July 22
W08	one	$\uparrow\downarrow$	260074 - 260264	July 23	July 29
	two	$\downarrow\uparrow$	260317 - 260565	July 29	August 5
W09	one	$\downarrow\uparrow$	260627 - 260852	August 5	August 12
	two	$\uparrow\downarrow$	260895 - 261496	August 12	August 26
W10	one	$\uparrow\downarrow$	261515 - 261761	August 26	September 1
	two	$\downarrow\uparrow$	261970 - 262221	September 4	September 9
W11	one	$\downarrow\uparrow$	262370 - 262772	September 11	September 22
	two	$\uparrow\downarrow$	262831 - 263090	September 23	September 30
W12	one	$\uparrow\downarrow$	263143 - 263347	September 30	October 7
	two	$\downarrow\uparrow$	263386 - 263603	October 8	October 14
W13	one	$\downarrow\uparrow$	263655 - 263853	October 15	October 21
	two	$\uparrow\downarrow$	263926 - 264134	October 22	October 28
W14	one	$\uparrow\downarrow$	264170 - 264330	October 28	November 2
	two	$\downarrow\uparrow$	264429 - 264562	November 4	November 8
W15	one	$\downarrow\uparrow$	264619 - 264672	November 9	November 11
	two	$\uparrow\downarrow$	264736 - 264857	November 12	November 16

Table 1.1 COMPASS 2015 data taking periods

as best primary (PHAST method `PaVertex::IsBestPrimary()`). If CORAL did not tag any of the common vertices as the best primary the vertex with the smallest spatial χ^2 value was used as the best primary vertex.

- A dimuon trigger fired. A dimuon trigger firing means there are at least two particles in coincidence in this event. The dimuon triggers used were a coincidence between two particles in the large angle spectrometer, LAS-LAS trigger, or a particle in the large angle spectrometer and a particle in the Outer hodoscope in the small angle spectrometer, LAS-Outer trigger. The LAS-Middle trigger was used a veto on beam decay muons. This is because the LAS-Middle trigger was found to have many events resulting from a beam pion decaying to a muon.
- Both particles are muons. A muon was defined as having crossed 30 radiation lengths of material between the particles first and last measured points. This criteria has been previously determined to be effective at distinguishing between muons and hadrons. In the final production no detectors were used from upstream of the hadron absorber so the absorber is not included in the determination of material crossed.

- The first measured point for both particles is before 300 cm and the last measured point is after 1500 cm. This cut ensures both particles have positions upstream of the first spectrometer magnet and downstream of the first muon filter.
- The timing of both muons is defined. This checks that the time relative to the trigger time is determined for both muons so further timing cuts can be performed.
- Both muons are in time within 5 nanoseconds. This cut helps rejected uncorrelated muons.
- The muon tracks reduced χ^2 are individually less than 10. This cut ensure track quality.
- A validation that each muon crossed the trigger it was associated as having triggered. This trigger validation cut was performed by extrapolating (PHAST Method `PaTrack::Extrapolate()`) each muon track back to the hodoscopes it fired and determining if the muon crossed the geometric acceptance of both hodoscopes.
- The event does not occur in the bad spill or run list.
- The Drell-Yan kinematics are physical. That is the beam and target x -Bjorken are between 0 and 1 and x -Feynman is between -1 and 1.
- The transverse momentum of the virtual photon is between 0.4 and 5.0 GeV/c. The lower limit ensures azimuthal angular resolution is sufficient and the upper cut is minimal and ensure physical kinematics.
- The vertex originated within the z-positions of the transversely polarized targets defined by the target group ($-294.5 < Z_{\text{vertex}} < -239.3$ or $-219.5 < Z_{\text{vertex}} < -164.3$ cm).
- The vertex is within the radius of the target defined as 1.9 cm.

Cuts	W07	W08	W09	W10	W11	W12	W13	W14	W15	WAll
All Data	19410	19184	19654	20707	31371	23563	20561	13154	7697	175301
Good Spills	15947	14899	16217	16895	23041	20184	16026	11796	7422	142427
$0 < x_\pi, x_N < 1, -1 < x_F < 1$	15932	14886	16200	16885	23022	20171	16013	11794	7414	142317
$0.4 < q_T < 5(\text{GeV}/c)$	14342	13385	14609	15239	20667	18101	14365	10588	6636	127932
Z Vertex within NH_3	4256	4024	4330	4552	6369	5503	4411	3130	2028	38603
Vertex Radius $< 1.9\text{cm}$	4175	3950	4257	4474	6252	5414	4334	3078	1987	37921

Table 1.2 Final event selection statistics

1.1.2 Binning

The final asymmetries are measured in bins of x_N , x_π , x_F , q_T , and $M_{\mu\mu}$. The binning was determined by requiring equal statistics per physics bin. In addition, the asymmetry is determined in integrated bin using all the final data. The final binning limits are summarized in table 1.3.

Kinematics	Lowest limit	Upper limit bin 1	Upper limit bin 2	Upper limit bin 3
x_N	0.0	0.13	0.19	1.0
x_π	0.0	0.40	0.56	1.0
x_F	-1.0	0.22	0.41	1.0
q_T (GeV/c)	0.4	0.86	1.36	5.0
$M_{\mu\mu}$ (GeV/c ²)	4.3	4.73	5.50	8.5

Table 1.3 Final binning limits

1.2 Extraction of Asymmetries

1.2.1 Geometric Mean

The number of physics counts, N , detected from any particular target with any polarization can be written as

$$N = L * \sigma * a, \quad (1.1)$$

where L is the luminosity, σ is the cross-section to produce such an event and a is the acceptance. In simple words, the number of counts detected is the number of chances for an event to occur times the probability for an event to occur and that the event will be detected. To get spin-dependent counts for the left, right asymmetry, the target, polarization and left

or right direction relative to the spin should be included in the counts formula. Generically this can be written

$$N_{\text{target,Left(Right)}}^{\uparrow(\downarrow)} = a_{\text{target,spectrometer direction}}^{\uparrow(\downarrow)} * L_{\text{target}}^{\uparrow(\downarrow)} * \sigma_{\text{Left(Right)}}, \quad (1.2)$$

where $\uparrow(\downarrow)$ denotes the target polarization, $_{\text{target}}$ is either the upstream or downstream target $_{\text{Left(Right)}}$ is left or right of the spin direction and $_{\text{spectrometer direction}}$ denotes which side of the spectrometer the event was detected on.

The previous definitions of the detected counts all depend on the spectrometer acceptance. This is a problem because the spectrometer acceptance can change with time and space and therefore can be dependent on the physical kinematics which produced the event. Such dependences can cause unphysical false asymmetries in the measurement of A_N and must therefore be removed or must be included as systematic effects.

The geometric mean asymmetry method is a way to determine the left, right asymmetry without acceptance effects from the spectrometer. It is defined as

$$\frac{1}{P} \frac{\sqrt{N_{\text{target,Left}}^{\uparrow} N_{\text{target,Left}}^{\downarrow}} - \sqrt{N_{\text{target,Right}}^{\uparrow} N_{\text{target,Right}}^{\downarrow}}}{\sqrt{N_{\text{target,Left}}^{\uparrow} N_{\text{target,Left}}^{\downarrow}} + \sqrt{N_{\text{target,Right}}^{\uparrow} N_{\text{target,Right}}^{\downarrow}}}, \quad (1.3)$$

where P represents the fraction of polarized partons.

Equation 1.3 can be thought of simply as the normalized difference of left minus right counts. Left and right counts are determined relative to the target spin and are defined as

$$\begin{aligned} \text{Left} : \hat{q}_T \cdot (\hat{S}_T \times \hat{P}_\pi) &> 0 \\ \text{Right} : \hat{q}_T \cdot (\hat{S}_T \times \hat{P}_\pi) &< 0, \end{aligned} \quad (1.4)$$

where \hat{q}_T , \hat{S}_T and \hat{P}_π are unit vectors in the target reference frame for the virtual photon transverse momentum, the target spin and the beam pion momentum respectively.

Using Eq. 1.2 for the definition of counts, the geometric mean asymmetry is

$$\frac{1}{P} \frac{\kappa \sqrt{\sigma_{Left} \sigma_{Left}} - \sqrt{\sigma_{Right} \sigma_{Right}}}{\kappa \sqrt{\sigma_{Left} \sigma_{Left}} + \sqrt{\sigma_{Right} \sigma_{Right}}}, \quad (1.5)$$

where κ is a ratio of acceptances defined as

$$\frac{\sqrt{a_{\text{target,Jura}}^{\uparrow} a_{\text{target,Saleve}}^{\downarrow}}}{\sqrt{a_{\text{target,Saleve}}^{\uparrow} a_{\text{target,Jura}}^{\downarrow}}}. \quad (1.6)$$

Here the detection side of spectrometer is specified by looking down the beam line as either Jura to mean left or Saleve to mean right. These relations of Jura is left and Saleve is right are only strictly true if in the target frame the polarization is pointing straight up or straight down. In particular if the beam particle and the target polarization do not make a right angle in the laboratory frame this relation will no longer be strictly true but is an approximation for ease of notation.

Relation 1.5 is equal to A_N if κ is equal to one. However as stated previously, time effects can vary κ from unity. These effects are estimated through false asymmetry analysis and included in the systematics. Equation 1.3 is therefore to a good approximation an acceptance free method to determine A_N . It is also defined for the upstream and downstream targets independently and therefore can be used as a consistency check between the two targets.

The statistical uncertainty of the geometry mean is

$$\frac{1}{P} \frac{\sqrt{N_{\text{Left}}^{\uparrow} N_{\text{Left}}^{\downarrow} N_{\text{Right}}^{\uparrow} N_{\text{Right}}^{\downarrow}}}{\left(\sqrt{N_{\text{Left}}^{\uparrow} N_{\text{Left}}^{\downarrow}} + \sqrt{N_{\text{Right}}^{\uparrow} N_{\text{Right}}^{\downarrow}} \right)^2} \sqrt{\frac{1}{N_{\text{Left}}^{\uparrow}} + \frac{1}{N_{\text{Left}}^{\downarrow}} + \frac{1}{N_{\text{Right}}^{\uparrow}} + \frac{1}{N_{\text{Right}}^{\downarrow}}}, \quad (1.7)$$

which reduces to $\frac{1}{P} \frac{1}{\sqrt{N}}$ in the case of equal statistics in each direction and polarization.

1.2.2 Four Target Geometric Mean

The previous method determined an A_N per target and as mentioned before COMPASS had two oppositely polarized targets in 2015. It would therefore makes sense from a statistical

point of view and for comparison purposes to determine A_N using all the information from the 2015 COMPASS setup. This can be accomplished by modifying the geometric mean to add all four targets as follows

$$\frac{1}{P} \frac{\sqrt[4]{N_{\text{up,Left}}^{\uparrow} N_{\text{up,Left}}^{\downarrow} N_{\text{down,Left}}^{\uparrow} N_{\text{down,Left}}^{\downarrow}} - \sqrt[4]{N_{\text{up,Right}}^{\uparrow} N_{\text{up,Right}}^{\downarrow} N_{\text{down,Right}}^{\uparrow} N_{\text{down,Right}}^{\downarrow}}}{\sqrt[4]{N_{\text{up,Left}}^{\uparrow} N_{\text{up,Left}}^{\downarrow} N_{\text{down,Left}}^{\uparrow} N_{\text{down,Left}}^{\downarrow}} + \sqrt[4]{N_{\text{up,Right}}^{\uparrow} N_{\text{up,Right}}^{\downarrow} N_{\text{down,Right}}^{\uparrow} N_{\text{down,Right}}^{\downarrow}}}. \quad (1.8)$$

Where up and down stand for the upstream and downstream targets respectfully.

As in the two target geometric mean, left and right are determined relative to the spin direction of the target as in Eq. 1.4. Again using Eq. 1.2 for the definition of counts, the four target geometric mean asymmetry, Eq. 1.8, can be written as

$$\frac{1}{P} \frac{\kappa \sqrt[4]{\sigma_{\text{Left}} \sigma_{\text{Left}} \sigma_{\text{Left}} \sigma_{\text{Left}}} - \sqrt[4]{\sigma_{\text{Right}} \sigma_{\text{Right}} \sigma_{\text{Right}} \sigma_{\text{Right}}}}{\kappa \sqrt[4]{\sigma_{\text{Left}} \sigma_{\text{Left}} \sigma_{\text{Left}} \sigma_{\text{Left}}} + \sqrt[4]{\sigma_{\text{Right}} \sigma_{\text{Right}} \sigma_{\text{Right}} \sigma_{\text{Right}}}}, \quad (1.9)$$

,

where now κ is the ratio of acceptances from all targets and polarizations. This all inclusive acceptance ratio is defined as

$$\frac{\sqrt[4]{a_{\text{up,Jura}}^{\uparrow} a_{\text{up,Saleve}}^{\downarrow} a_{\text{down,Jura}}^{\uparrow} a_{\text{down,Saleve}}^{\downarrow}}}{\sqrt[4]{a_{\text{up,Saleve}}^{\uparrow} a_{\text{up,Jura}}^{\downarrow} a_{\text{down,Saleve}}^{\uparrow} a_{\text{down,Jura}}^{\downarrow}}}. \quad (1.10)$$

Finally the statistical uncertainty of the four target geometric mean is

$$\frac{1}{P} \frac{LR}{(L+R)^2} \sqrt{\sum_{\text{target}} \sum_{\text{polarization}} \left(\frac{1}{N_{\text{target,Left}}^{\text{polarization}}} + \frac{1}{N_{\text{target,Right}}^{\text{polarization}}} \right)}, \quad (1.11)$$

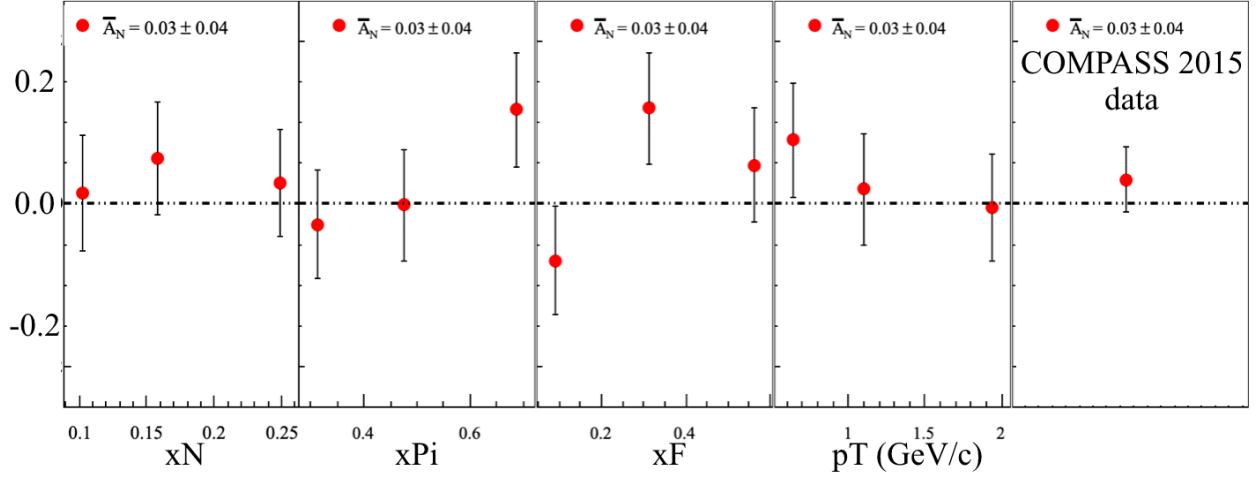
where L can be thought of as the left counts and equals to $\sqrt[4]{N_{\text{up,Left}}^{\uparrow} N_{\text{up,Left}}^{\downarrow} N_{\text{down,Left}}^{\uparrow} N_{\text{down,Left}}^{\downarrow}}$ and R can be thought of as the right counts and equals $\sqrt[4]{N_{\text{up,Right}}^{\uparrow} N_{\text{up,Right}}^{\downarrow} N_{\text{down,Right}}^{\uparrow} N_{\text{down,Right}}^{\downarrow}}$. The statistical uncertainty for the four target geometric mean also reduces to $\frac{1}{P} \frac{1}{\sqrt{N}}$ in the case of equal statistics in each direction and polarization.

1.3 Results

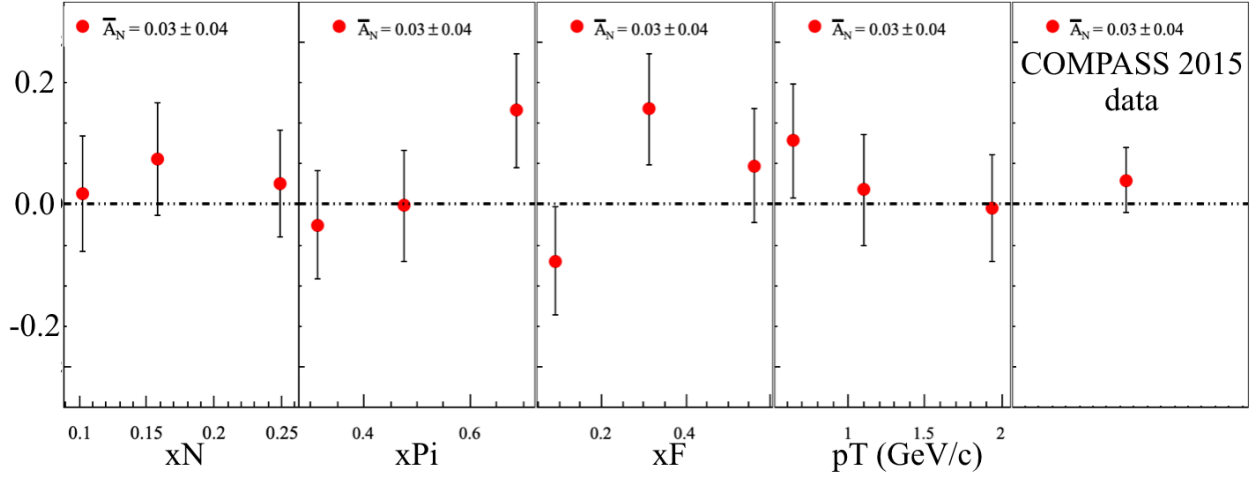
The final asymmetries are calculated from each of the separate nine periods and then combined as a weighted average. This method for calculating is used to minimize the effects of acceptance changes between periods as the spectrometer was kept stable within each period but had the options for detector changes between periods. This final weighted is determined as

$$A_N = \sum_{\text{period}} \frac{A_{N,\text{period}} \sigma_{\text{period}}^{-2}}{\sigma_{\text{period}}^{-2}}, \quad \sigma^2 = \sum_{\text{period}} \frac{1}{\sigma_{\text{period}}^{-2}}. \quad (1.12)$$

The final results for the two target geometric mean are show in Fig. 1.1 and the final results for the four target geometric mean and shown in Fig. 1.2. The systematic error bars are discussed in Sec. 1.4.



Figs 1.1 A_N determined from the geometric mean method for each target



Figs 1.2 A_N determined by the geometric mean method using all targets simultaneously

1.3.1 Comparison of results

1.4 Systematic Studies

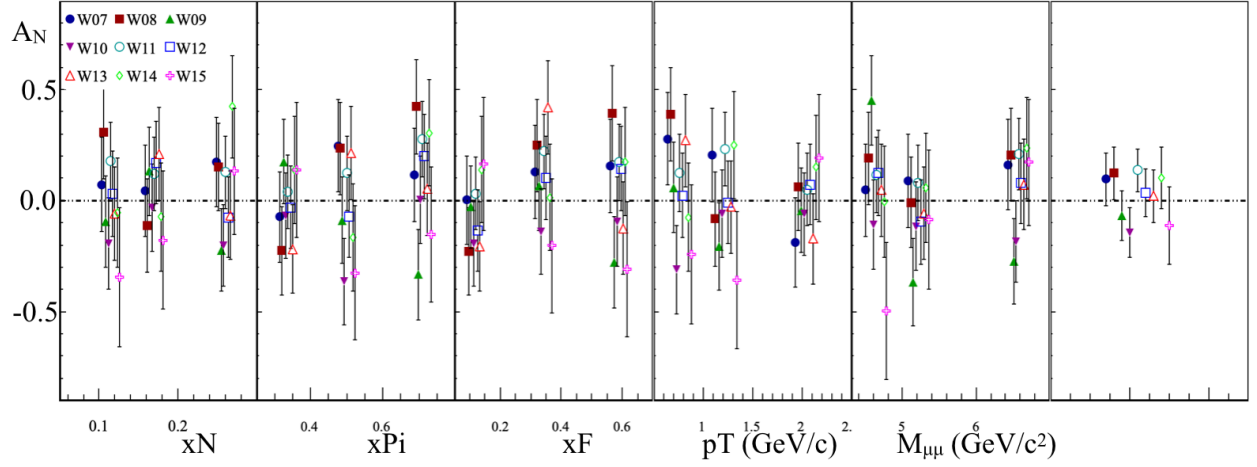
Several tests were performed to estimate the systematic uncertainty. The final systematic errors are determined by adding all non-zero systematic effects in quadrature. The impact from each source of systematic error is summarized in Tab. 1.4. List all test/systematic performed.....

1.4.1 Period Compatibility

The asymmetry calculated for each period in each kinematic bin is shown in Fig. ??.

By eye the asymmetry fluctuations appear to be statistically compatible. To quantify the compatibility of the asymmetries between the periods, a pull distribution is formed. The pull value is defined as

$$\Delta A_i = \frac{A_i - \langle A \rangle}{\sqrt{\sigma_{A_i}^2 - \sigma_{\langle A \rangle}^2}}, \quad (1.13)$$



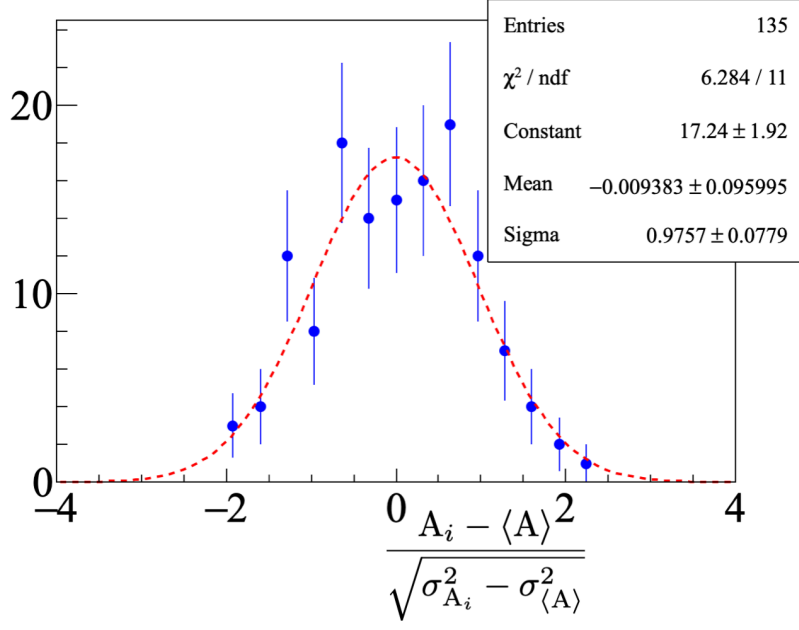
Figs 1.3 A_N determined for each period

and is determined for each period and kinematic bin. There are therefore $3(\text{number of bins}) \times 5(\text{number of kinematics}) \times 9(\text{number of periods}) = 135$ entries in the pull distribution. This distribution is shown in Fig. 1.4 along with a Gaussian fit. If the asymmetries all come from the same parent distribution then the pull distribution will be a Gaussian distribution with zero mean and unit variance. The discrepancy of the pull distribution from a standard Gaussian distribution is used to determine systematic error as

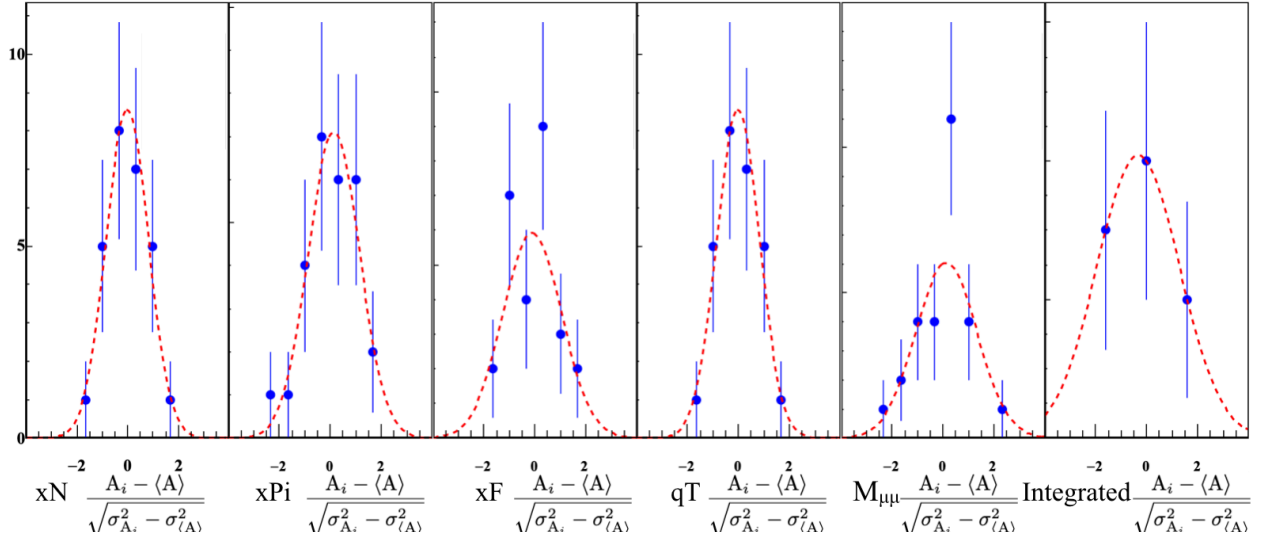
$$\frac{\sigma_{\text{systematic}}}{\sigma_{\text{statistical}}} = \sqrt{|\sigma_{\text{pull}}^2 - 1|} + \frac{\mu_{\text{pull}}}{2}. \quad (1.14)$$

As the asymmetries in different kinematic bins are formed using the same data set the asymmetries between kinematics are correlated. For this reason an uncorrelated pull distribution is formed for each physics kinematic bin and also compared with a standard Gaussian distribution. These distributions are shown in Fig. 1.5 where there are now only $3(\text{number of bins}) \times 9(\text{number of periods}) = 27$ entries in each of the pull distributions.

The final systematic error from compatibility is...



Figs 1.4 Pull distributions



Figs 1.5 Pull distributions

1.4.2 False Asymmetries

Acceptance From False Asymmetries

As was pointed out in Sec. 1.2.1 and Sec. 1.2.2, the asymmetry measurement assumes the acceptance does not change with time and therefore the acceptance ratios Eq. 1.6 and Eq. 1.10 are unitary. Any deviation from unitary acceptance ratios is estimated with a false asymmetry and the errors are included as systematic errors. To determine if acceptance does change with time, a false asymmetry is calculated where the only way the false asymmetry could be non-zero is if acceptance changes with time. This false asymmetry for the four target geometric mean is

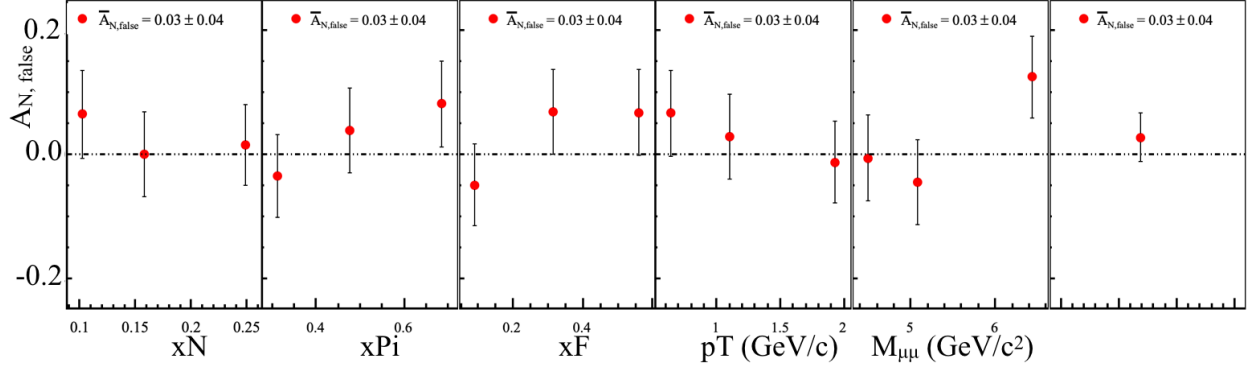
$$\begin{aligned}
A_{N, \text{False}} &= \frac{1}{P} \frac{\sqrt[4]{N_{\text{up,Right}}^{\uparrow} N_{\text{up,Left}}^{\downarrow} N_{\text{down,Left}}^{\uparrow} N_{\text{down,Right}}^{\downarrow}} - \sqrt[4]{N_{\text{up,Left}}^{\uparrow} N_{\text{up,Right}}^{\downarrow} N_{\text{down,Right}}^{\uparrow} N_{\text{down,Left}}^{\downarrow}}}{\sqrt[4]{N_{\text{up,Right}}^{\uparrow} N_{\text{up,Left}}^{\downarrow} N_{\text{down,Left}}^{\uparrow} N_{\text{down,Right}}^{\downarrow}} + \sqrt[4]{N_{\text{up,Left}}^{\uparrow} N_{\text{up,Right}}^{\downarrow} N_{\text{down,Right}}^{\uparrow} N_{\text{down,Left}}^{\downarrow}}} \\
&= \frac{1}{P} \frac{\alpha \sqrt[4]{\sigma_{\text{Right}} \sigma_{\text{Left}} \sigma_{\text{Left}} \sigma_{\text{Right}}} - \sqrt[4]{\sigma_{\text{Left}} \sigma_{\text{Right}} \sigma_{\text{Right}} \sigma_{\text{Left}}}}{\alpha \sqrt[4]{\sigma_{\text{Right}} \sigma_{\text{Left}} \sigma_{\text{Left}} \sigma_{\text{Right}}} + \sqrt[4]{\sigma_{\text{Left}} \sigma_{\text{Right}} \sigma_{\text{Right}} \sigma_{\text{Left}}}} \\
&= \frac{1}{P} \frac{\alpha - 1}{\alpha + 1},
\end{aligned} \tag{1.15}$$

where α is an acceptance ratio and is defined as

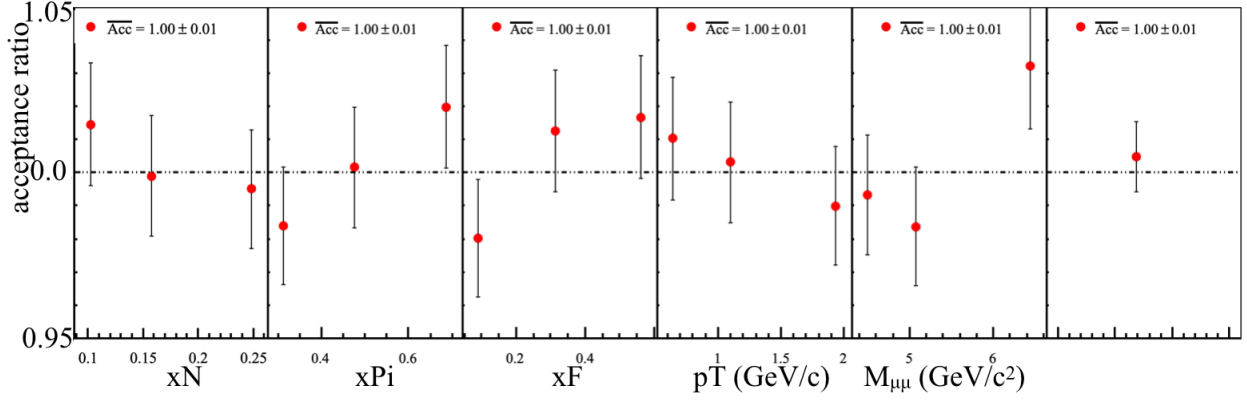
$$\frac{\sqrt[4]{a_{\text{up,Saleve}}^{\uparrow} a_{\text{up,Saleve}}^{\downarrow} a_{\text{down,Jura}}^{\uparrow} a_{\text{down,Jura}}^{\downarrow}}}{\sqrt[4]{a_{\text{up,Jura}}^{\uparrow} a_{\text{up,Jura}}^{\downarrow} a_{\text{down,Saleve}}^{\uparrow} a_{\text{down,Saleve}}^{\downarrow}}}. \tag{1.16}$$

The kinematic dependencies of the false asymmetry are shown in Fig. 1.6 and the kinematic dependencies of the acceptance ratio, α , are shown in Fig. 1.7.

While α is an acceptance ratio it is not the same as the acceptance ratio in the true asymmetry. However α is similar to the true acceptance ratio, κ , in that α will only be different from unity as a result of time changes in the spectrometer. Therefore it is assumed α can be used as a good estimate of the true acceptance ratio. The systematic error due to acceptance fluctuations is determined as



Figs 1.6 False asymmetry to estimate fluctuations in acceptance in time



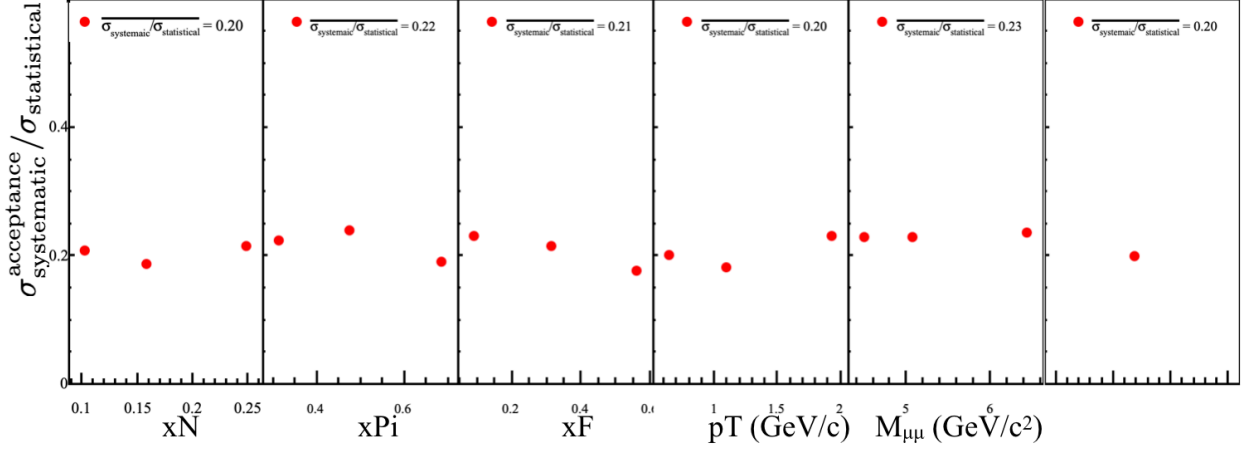
Figs 1.7 Acceptance ratio used to determine the systematic effects from acceptance changes in time

$$\delta A_{N,\text{systematic}} = \frac{1}{P} \left(\frac{|\alpha - 1|}{2} + \delta_{\frac{|\alpha-1|}{2}} \right). \quad (1.17)$$

The kinematic dependence of the systematic error normalized to the statistical error is shown in Fig. 1.8. The binned average systematic error due to acceptance is 20% of the statistical error.

1.4.3 Further False Asymmetry Effects

Although the list of systematic effects specifically studied is quite exhaustive there is always the potential for other systematic effects not considered. Studies of the changes in time from additional false asymmetries were performed in an attempt to take into account all these other



Figs 1.8 Systematic error due to acceptance effects

systematic effects. All false asymmetries considered must be constructed in such a way that the physical process of interest cancels out. A false asymmetry could therefore only be non-zero from acceptance effects, luminosity or some other reason not considered. The additional false asymmetries constructed made in a way that luminosity effects canceled out and acceptance effects were approximately constant. With these assumptions pull values from Eq. 1.13 should form a standard Gaussian distribution. Any deviation from a standard Gaussian is conservatively taken as a systematic effect from some unknown cause. The additional studied false asymmetries are summarized in the following 1.4.3.

1. A false asymmetry similar to Eq. 1.15 but with left and right counts shifted defined in Eq. 1.18.

$$\frac{1}{P} \frac{\sqrt[4]{N_{\text{up,Left}}^{\uparrow} N_{\text{up,Right}}^{\downarrow} N_{\text{down,Left}}^{\uparrow} N_{\text{down,Right}}^{\downarrow}} - \sqrt[4]{N_{\text{up,Right}}^{\uparrow} N_{\text{up,Left}}^{\downarrow} N_{\text{down,Right}}^{\uparrow} N_{\text{down,Left}}^{\downarrow}}}{\sqrt[4]{N_{\text{up,Left}}^{\uparrow} N_{\text{up,Right}}^{\downarrow} N_{\text{down,Left}}^{\uparrow} N_{\text{down,Right}}^{\downarrow}} + \sqrt[4]{N_{\text{up,Right}}^{\uparrow} N_{\text{up,Left}}^{\downarrow} N_{\text{down,Right}}^{\uparrow} N_{\text{down,Left}}^{\downarrow}}} \quad (1.18)$$

1.4.4 Left/Right Event Migration

Systematic error	$\langle \sigma_{\text{systematic}} / \sigma_{\text{statistical}} \rangle$
Period compatibility	0.0
Acceptance fluctuation	0.2
Total	0.0

Table 1.4 Summary of systematic error impacts to the integrated asymmetry

List of Figures

1.1	A_N determined from the geometric mean method for each target	8
1.2	A_N determined by the geometric mean method using all targets simultaneously	9
1.3	A_N determined for each period	10
1.4	Pull distributions	11
1.5	Pull distributions	11
1.6	False asymmetry to estimate fluctuations in acceptance in time	13
1.7	Acceptance ratio used to determine the systematic effects from acceptance changes in time	13
1.8	Systematic error due to acceptance effects	14

List of Tables

1.1	COMPASS 2015 data taking periods	2
1.2	Final event selection statistics	4
1.3	Final binning limits	4
1.4	Summary of systematic error impacts to the integrated asymmetry	15

listed in References

Chapter 2

References